Shear Thinning Effects by VII Added Lubricant with In-Situ Optical Viscometer

장 시 열†

Siyoul Jang†

Key Words : elastohydrodynamic lubrication (EHL), in-situ EHL optical interferometer (optical viscometer), viscosity index improver, shear thinning, multigrade lubricant

Abstract

Viscosity index improver (VII) is one of the major additives to the modern multigrade lubricants for the viscosity stability against temperature rise. However, it causes shear thinning effects which make the film thickness lessened very delicately at high shear rate (over $10^5\ s^{-1}$) of general EHL contact regime. In order to exactly verify the VII's performance of viscosity stability at such high shear rate, it is necessary to make the measurement of EHL film thickness down to ~100*nm* with fine resolution for the preliminary study of viscosity control. In this work, EHL film thickness of VII added lubricant is measured with the resolution of ~5*nm*, which will give very informative design tool for the synthesis of lubricants regarding the matter of load carrying capacity at high shear rate condition.

1. INTRODUCTION

In-situ EHL optical interferometric technology (that is, optical viscometer) for measuring the film thickness is very useful method in the investigations of rheological properties of lubricant at high shear rate and high applied load. It simulates most of contact geometries, materials and lubrication conditions by changing the contact curvatures of radius, equivalent of elastic modulus, starvation or flooded boundary conditions. In particular, it can provide the visualization of the EHL film thickness images all over the contact area in the studies by Bair (1995), Williamson (1995) and Smeeth et al. (1995). Another great advantage of this in-situ EHL optical measuring technology is that it can test various contact velocities (or shear strain rates) up to 108 s-1, which most severe contact environments in precision elements of machinery have.

Digital image processing technology by Krupka et al. (1997) also enhances the performance of in-situ optical EHL interferometric method by giving consistent and objective interpretation tool of measured film thickness over the contact area with very fine resolution of ~10nm. Without the developed technology, only central and minimum film thickness might be concerned, which makes the interpretation of measure film thickness by naked eye much biased to the observer's experiences.

In this work, minute changes of EHL film thickness with VII added condition are investigated for the preliminary study of lubricant synthesis design with various kinds of contact velocities and loads down to ~100nm of EHL film thickness. The investigations are performed by in-situ EHL optical interferometric apparatus and image processing technology with less than ~5nm scale of film thickness previously developed by the author.

2. APPARENT VISCOSITY CHANGE BY THE VISCOSITY INDEX IMPROVER

Viscosity index improver in the multigrade lubricant is used against the rapid drop of viscosity at working temperature rising up to 150°*C*. Many precision contacts of mechanical elements such as cam-tappet in automobile engine and ball-race in precision rolling contact bearings have severe contact behaviors of elastohydrodynamic lubrication regime which have both high shear rate modes over $10^5\ s^{-1}$ and high pressure over 1.0 *GPa* in general. However, the viscosity stability by

† 국민대학교 기계· 자동차공학부
E-mail : jangs@kookmin.ac.kr
TEL : (02)910-4831 FAX : (02)910-4839

long chained polymeric molecular structure of VII against temperature rise is delicately influenced by such high shear rate with thin fluid film (~0.1 μm), which is common working condition of precision machinery. At such high shear rate where high concentrated normal pressure on the contact area is accompanied, the polymeric molecules are aligned along the sliding direction and subsequently the apparent viscosity (or shear resistance) is lessened in thin film status under high normal pressure. This is the reason that the load carrying capacity of lubricant with VII containing long chained polymeric molecules is far smaller than pure base oil under the condition of the same applied load as shown in the work by Bird et al. (1987) and Harris (1977).

The fluid film pressure in the contact area is described by the following Reynolod's equation with respect of continuum mechanics by Hamrock (1994).

$$\frac{\partial}{\partial x}\left(\frac{\rho h^3}{12\eta}\frac{\partial p}{\partial x}\right)+\frac{\partial}{\partial y}\left(\frac{\rho h^3}{12\eta}\frac{\partial p}{\partial y}\right)-u\frac{\partial(\rho h)}{\partial x}=0 \qquad (1)$$

where the viscosity $\eta = f\left(\frac{d\gamma}{dt}, p\right)$ has the functions of shear rate and applied pressure.

The load capacity by the fluid film pressure is computed by the summation of pressure over the contact area as shown below.

$$W = \int_A p(x,y)dxdy \qquad (2)$$

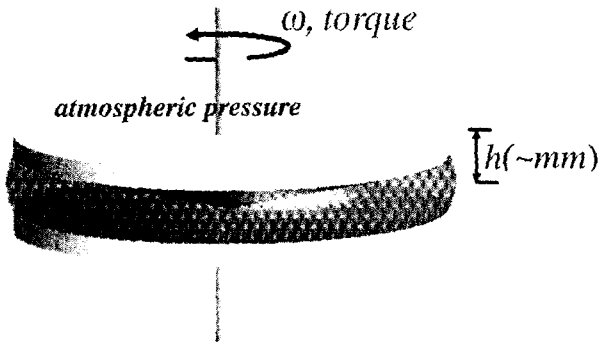

Figure 1 Viscosity measurement according to the variation of shear strain rate by cone and plate viscometer (Paar-Physica UM)

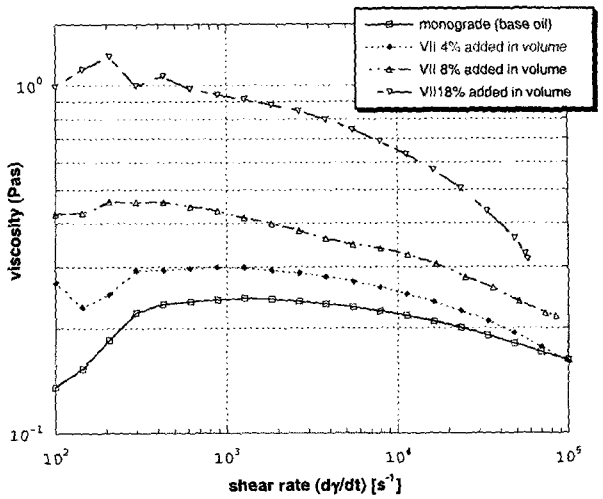

Figure 2 Viscosity variations according to portion of the viscosity index improver by cone and plate viscometer (Paar-Physica UM) up to $10^5\ s^{-1}$ of shear strain rate

Conventional viscometer like cone-plate rheometry system, Figure 1 measures the viscosity by sensing the shear resistance with rotating two thin-separated plates (~1mm). This measurement can easily verify the viscosity changes according to shear rates less than ~$10^5\ s^{-1}$. However, the measurement range of shear strain rate by cone-plate viscometer is still much lower than that of actual contacts of precision mechanical elements and does not give informative design parameters for the blending of lubricant. What is less, it measures the viscosity values only under the condition of atmospheric pressure where the true viscosity performance of lubricant cannot be verified at all under the real contact environment.

Viscosity variations are measured in this study according to cone-plate viscometer (Paar-Physica UM) where the testing range of shear strain rate is possible up to $10^5\ s^{-1}$ at most. This is the range far below shear rate in the real contacts of precision mechanical elements and it provides only the results of atmospheric pressure, while most precision mechanical elements undergo pressures over 1.0 GPa and shear strain rates over $10^5\ s^{-1}$, respectively. Viscosity changes by the additions of VII to base oil are measured by cone and plate viscometer as shown in Figure 2. Addition of VII to base oil makes the lubricant more viscous, but the viscosity of each case decreases as the shear rate increases.

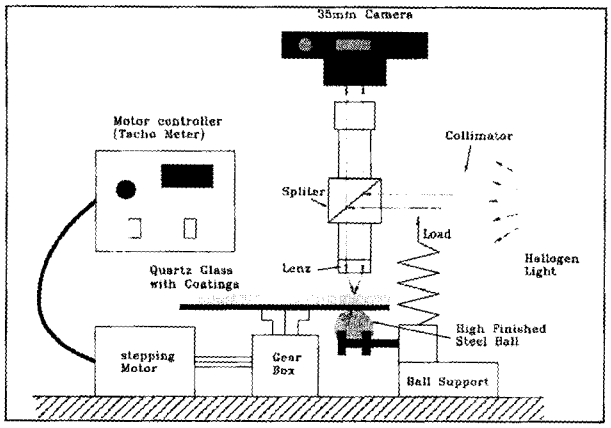

Figure 3 Schematic diagram of in-situ EHD optical interferometer (optical viscometer) for film measurement

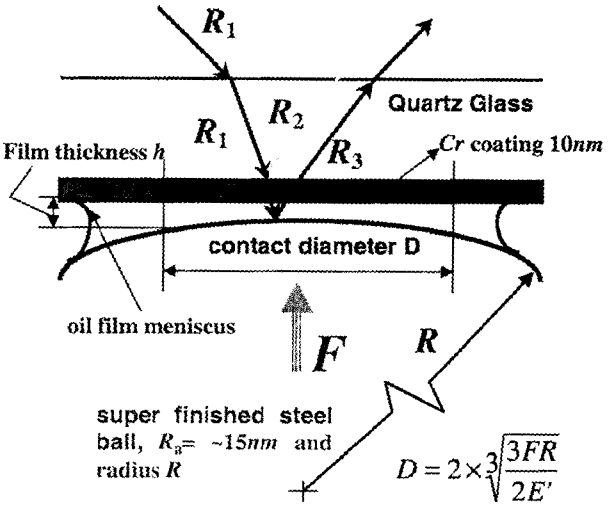

Figure 4 Reflected beams on *Cr* coating surface (half mirror) and steel ball

The higher portion of VII in the blended lubricant (multigrade libricant), the more rapid drop of viscosity as the shear rates increase. This is the general tendency when VII is added even under atmospheric pressure. Further increase of shear rate in cone and plate viscometer for the viscosity measurement of EHL regime needs much thinner contact of ~μm gap between cone and plate or increase rotational speed of cone. However, this is not simple problem with the respects of parallel control of ~μm gap between cone and plate which might has a relatively large contact area of ~2000mm^2 scale as well as rotational inertia control of tested lubricant by dissipated effect.

In order to verify the performance of long chained polymeric VII under the condition of high shear rate and high pressure for the high-performance lubricant design, it is necessary to make the precision measurement of contact film thickness, contact velocity and applied load at the same time. Although the measurement of contact velocity and applied load are easily obtainable by sensing the speed of driving motor and the kinematic contact geometry, respectively, the measurement of film thickness needs much precision for fine resolution in both normal and shearing orientations of contact.

In-situ EHL optical interferometric method makes it possible to make the measurement of area size of contact spot as well as film thickness ranging from 100nm to 2μm with ~5nm resolution over the contact area.

The measured contact size provides the information of applied load, material modulus and contact geometry, because the kinematic geometry of in-situ EHL contact feature realizes the contact behaviors in precision elements of machinery. The viscosity characteristics to any shear rates under high pressure up to ~1.5GPa can be verified by the captured interferometric image of EHL film thickness in fine resolution only with the measurement of rotational torque.

The pattern of EHL film thickness also provides informative pressure-viscosity characteristics of tested lubricant that cannot be obtained by other methods with such simple way.Many other advantages of in-situ EHL optical viscometer over the conventional high shear rate viscometers are the followings:

1) Conventional high shear rate viscometer operates only at atmospheric pressure which cannot consider the high concentrated effect of pressure.

2) It generates heat and it is difficult to determine true oil temperature.

3) In real contact of machinery such as cam-tappet contact, the lubricant undergoes intermittent shear once per revolution of the cam, while the conventional high shear viscometer is subjected to prolonged shearing during the test.

In this experimental work of load carrying capacity of VII added lubricants, in-situ EHL apparatus for measuring the interference images of

EHL film thickness with VII added lubricants is developed as well as color-film thickness chart in terms of *CIE LAB* under the condition of white incident light are made. The developed system can make the measurement of EHL film thickness with ~5*nm* resolution. The performance of the optical interference method is very strongly dependent on the coating layer on the transparent glass whose thickness are coated with around 10*nm* thickness of *Cr* layer on the highly transparent glass of 150*mm* diameter (Figure 3). White light is filtered with day light filter that can pass all frequencies of visible colors and fine finished steel ball of 25 *mm* diameter with the roughness of R_a, 15*nm* scale are used so that the incident light can be reflected by 25% of after the *Cr* layer in order to get the most distinct resolution without any noise (Figure 4).

Schematic diagram of the developed device and the mechanism of incident light reflection are shown in Figure 3 and 4. The elastic modulus and Poisson's ratios of glass and ball are $E_b = 207 \times 10^9$ N/m^2, E_d = 76310^9 N/m^2, ν_b = 0.30, ν_d =0.25, respectively.

3. EHL FILM THICKNESS-COLOR CHART BY IMAGE PROCESSING METHOD UNDER WHITE INCIDENT LIGHT

Every pixel in the color interferogram outside of Hertzian contact circle as shown in Figure 5 is decomposed into RGB values, which are subsequently converted into L^*, $a^*$and b^* values for the calibration of film thickness (Figure 6).

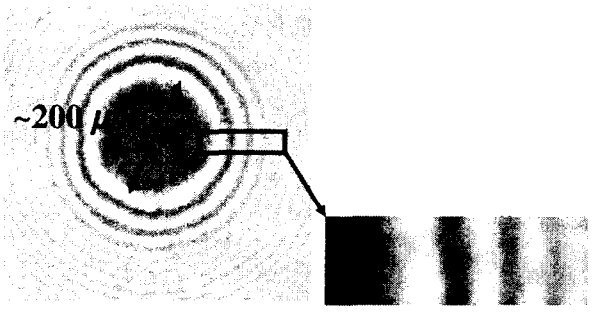

Figure 5 Interferogram of white incident light with 10*N* static load and color changes at the fringe boundaries as the film thickness changes

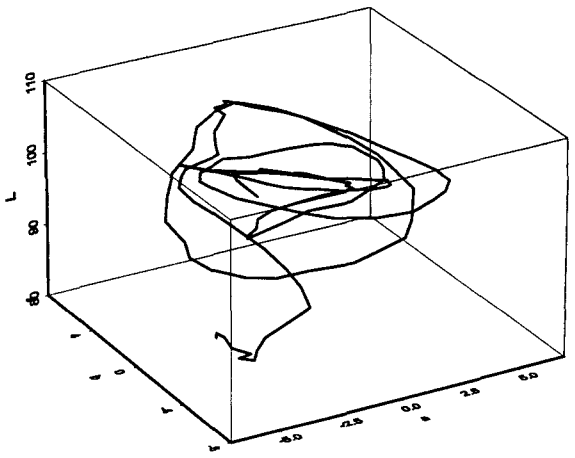

Figure 6 Spatial color coordinates of $L^*a^*b^*$ by white incident light in the range of 100~700*nm* of EHL film thickness

The film thickness outside of Hertzian contact area is obtainable by numerical computation of Hertzian contact theory. The EHL film thickness-color chart is then obtained by matching the L^*, $a^*$and b^* values with the gap between steel ball and glass plate from Hertzian contact theory. (Figure 7) In this experimental study, EHL film thickness can be fully investigated with the developed chart in the range from 100*nm* to 700*nm* all over the contact area, which cannot be accessible with other measuring systems such as capacitance gap sensor, infrared light and any other spectrometers measuring only single large spot (~*mm* diameter size) in the Hertzian contact area.

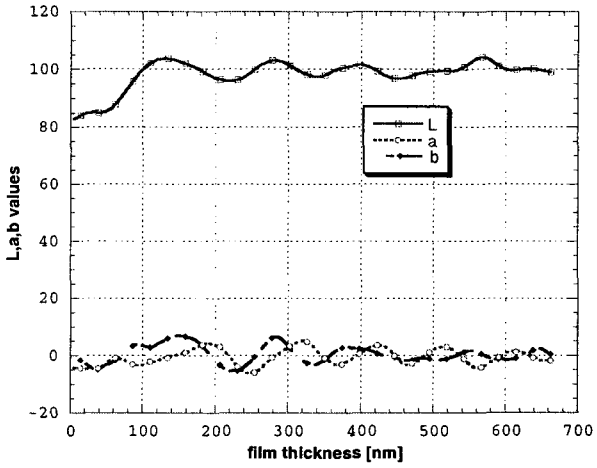

Figure 7 Film thickness-color chart for EHL contact by white incident light

Once the EHL film thickness-color chart is made as in Figure 7, every $L^*a^*b^*$ formatted pixel in the captured color interferogram of EHL film thickness is compared with the chart. In order for the selected pixel to get the nearest value to the computed $L^*a^*b^*$ chart, sweeping all over the captured pixels with the minimization of color difference ΔE^*_{ab} is performed by the following color difference equation by Krupka *et al.* (1997).

$$\Delta E^*_{ab} = \left[(\Delta L^*)^2 + (\Delta a^*)^2 + (\Delta b^*)^2\right]^{1/2} \quad (3)$$

With both the developed experimental apparatus and the image processing technology, minute variations of EHL film thickness less than ~5*nm* film thickness according the addition of VII to base oil can be detectable at high shear rate over $10^5\ s^{-1}$ with consistency and objectivity.

4. RESULTS

The viscosity of the lubricant under atmospheric pressure, ambient temperature 20°*C* and ~$10^2\ s^{-1}$ shear rate is measured around ~1.0 *Pas* by cone and plate viscometer (Figure 2). Under the condition of ambient temperature and pressure (~10^{-4} *GPa*) with low shear rate around ~$10^2\ s^{-1}$, the viscosity of the blended lubricant has higher values as the portion of VII in the base oil. This is taken for granted because VII is much more viscous than base oil in general. However, higher shear rate over $10^5\ s^{-1}$ makes the viscosity decrease rapidly as more VII is added to the base oil. That is, higher tendency of shear thinning behavior becomes with more VII added to base oil even under ambient temperature.

Table 1 Properties of tested base oil and viscosity index improver

test items	method	base oil	VII
Density @15°C	ASTM D 1298	0.8897	0.8943
Color(ASTM)	ASTM D 1500	L1.5	L0.5
Kin. Vis 40°C (cSt)	ASTM D 445	95.09	-
Kin.Vis 100°C(cSt)	ASTM D 445	10.85	534
Pour Point °C	ASTM D 97	-15	-
Flash Point °C	ASTM D 92	242	-
TBN, mgKOH/g	ASTM D 2896	-	-

Table 2 Selected four cases out of 55 tested conditions in in-situ EHL interferometer

selected test cases	lubricant	applied load [N]	contact velocity [m/s]
case I	base oil	10N	0.08233 m/s
case II	base oil	15N	0.0382 m/s
case III	base oil + VII 18%	10N	0.06586 m/s
case IV	base oil + VII 18%	15N	0.06586 m/s

Under the contact of high normal stress over 0.5 *GPa* and high shear rate over $10^5\ s^{-1}$ where EHL contact occurs, shear thinning effect is more vivid than the tested results by cone and plate viscometer.

The developed in-situ EHL optical interferomtry of EHL contact can verify the shear thinning behaviors under various contact loads and velocities by capturing the images of contact spot. In this work, the calibration data for the range of image processed film thickness is set up into EHL film thickness-color charts (Figure 6 and 7). According to the obtained EHL film thickness-color charts, the film thickness can be digitally processed in the range of 100*nm*~700*nm* with the resolution of ~5*nm* over the contact area depending on the noise in the captured images and the incident light. The captured optical interferogram images of EHL film thickness over the Hertzian contact area are converted into digitally formatted pixel such as CIE $L^*a^*b^*$ and compared with EHL film thickness-color chart pixel by pixel. The film thickness on each pixel is then obtained all over the contact area if it is in the range of 100*nm*~700*nm*.

The developed image processing method is applied to the cases of VII (Table 1) effects on the load carrying performances by changing applied loads and rolling contact velocities. Four cases (Table 2) are selected out of 55 tested results with base oil and blended VII lubricant by changing contact loads and velocities. Normal contact loads of 10*N* (P_h=0.58 *GPa*, *a*=92.58 *μm*) to 15 *N* (P_h=0.64 *GPa*, *a*=105.98 *μm*)are applied and rolling contact velocities of from 0.15 *m/s* to 0.015 *m/s* are

tested, respectively. Regarding the cases of base oil (monograde oil), the EHL film thickness fully takes the principle from theoretical investigations that high load and low contact velocity make the fluid film thickness thin. Film thickness of monograde oil with 10*N* load and 0.08233 *m/s* contact velocity is obtained in Figure 8 and 9 (Case I).

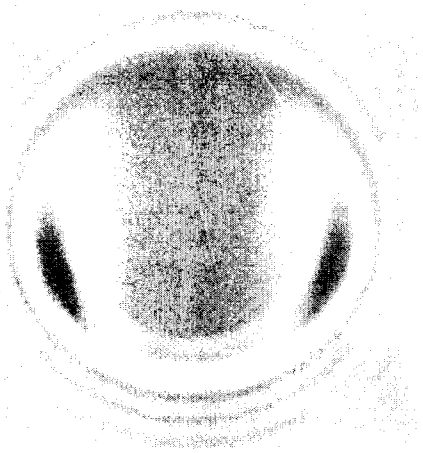

Figure 8 Interferometric image of base oil under the load of 10*N* and rolling speed of 0.08233*m/s* (Case I)

In case I, the minimum film thickness is around ~250*nm*. Higher load and lower contact velocity (10*N*, 0.03820 *m/s*, case II) are applied to monograde oil to compare with the previous case I. Case II (Figure 10 and 11) give minimum film thickness around ~150 *nm* thinner by ~100*nm* than case I. These experimental results agree well with theoretical studies by many other previous researches by the works, Greenwood (1988), Hamrock (1994), Evans *et al.* (1986).

EHL film thicknesses of VII added lubricant are also measured in the same way. Contact load of 10*N* and rolling contact velocity of 0.06586 *m/s* (case III), and higher contact load (15*N*) and same rolling contact velocity of 0.06586 *m/s* (case IV) are tested.

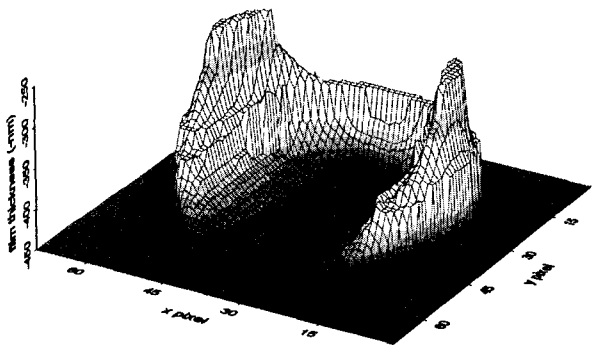

Figure 9 Image processed film thickness of base oil under the load of 10*N* and rolling speed of 0.08233*m/s* (Case I)

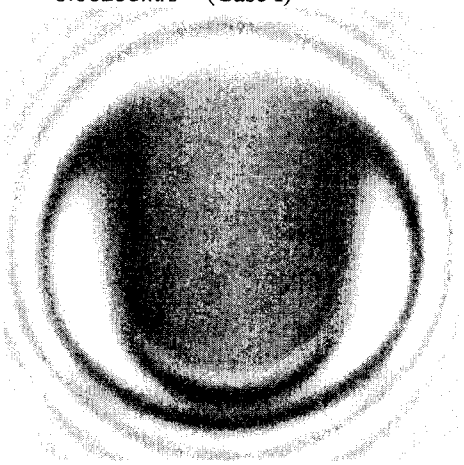

Figure 10 Interferometric image of base oil under the load of 15*N* and rolling speed of 0.03820*m/s* (Case II)

Case III gives minimum film thickness of 240*nm* (Figure 12 and 13), while case IV (Figure 14 and 15) does minimum film thickness of 200 *nm*. All the images of measured film thicknesses are digitally processed with 5*nm* resolution by the developed technology in this work and the capability to verify the magnitude of film thickness is shown in Figure 16 that is the centerline film thickness of Figure 11(Case II). EHL film thicknesses of VII added lubricant are also measured in the same way. Contact load of 10*N* and rolling contact velocity of 0.06586 *m/s* (case III), and higher contact load (15*N*) and same rolling contact velocity of 0.06586 *m/s* (case IV) are tested. Case III gives minimum film thickness of 240*nm* (Figure 12 and 13), while case IV (Figure 14 and 15) does minimum film thickness of 200 *nm*.

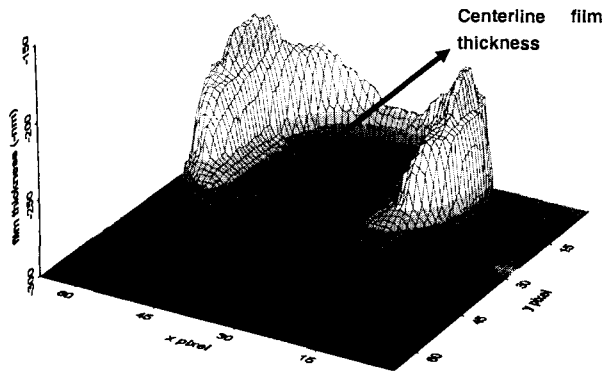

Figure 11 Image processed film thickness of base oil under the load of 15*N* and rolling speed of 0.03820*m/s* (Case II)

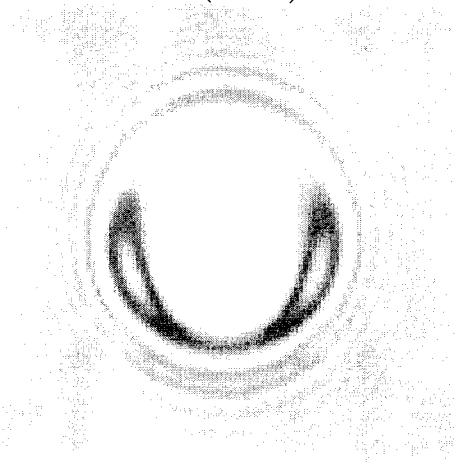

Figure 12 Interferometric image of VII added lubricant (18%) under the load of 10*N* and rolling speed of 0.06586*m/s* (Case III)

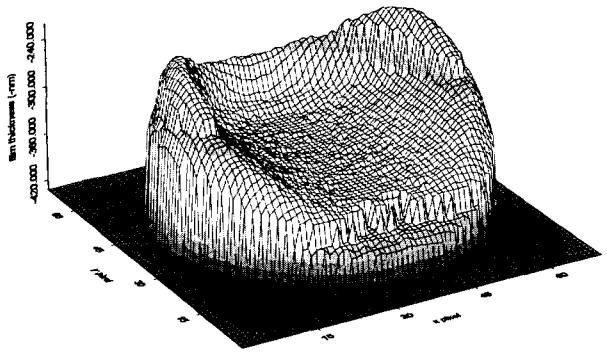

Figure 13 Image processed film thickness of VII added lubricant (18%) under the load of 10*N* and rolling speed of 0.06586*m/s* (Case III)

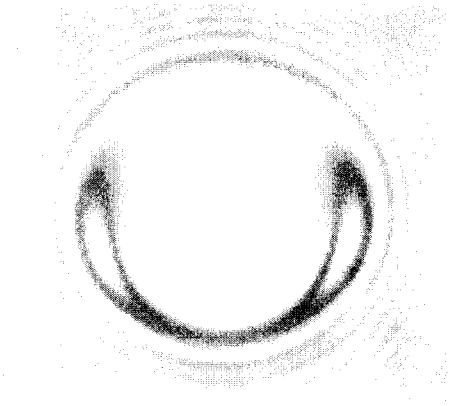

Figure14 Interferometric image of VII added lubricant (18%) under the load of 15*N* and rolling speed of 0.06586*m/s* (Case IV)

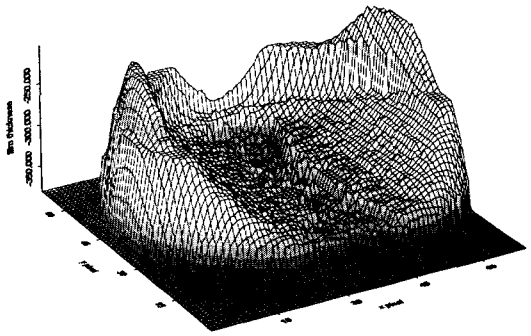

Figure 15 Image processed film thickness of VII added lubricant (18%) under the load of 15*N* and rolling speed of 0.06586*m/s* (Case IV)

All the images of measured film thicknesses are digitally processed with 5*nm* resolution by the developed technology in this work and the capability to verify the magnitude of film thickness is shown in Figure 16 that is the centerline film thickness of Figure 11(Case II).

We also expand the experimental ranges of contact load and velocities (Figure 17) for Case I, II, III and IV. The load capacities of monograde oil (case I and II) are higher than those of VII added lubricant (case III and IV) under the same contact condition by ranging from ~10 *nm* to ~40*nm* of film thickness scale. Without the developed image processing technology of fine resolution (~5 *nm*) for EHL film interferogram, these finding that load carrying capacity minutely changes at high shear rate (contact velocity/measured minimum film thickness in the contact area) over $10^5\ s^{-1}$ under VII added condition cannot be verified at all.

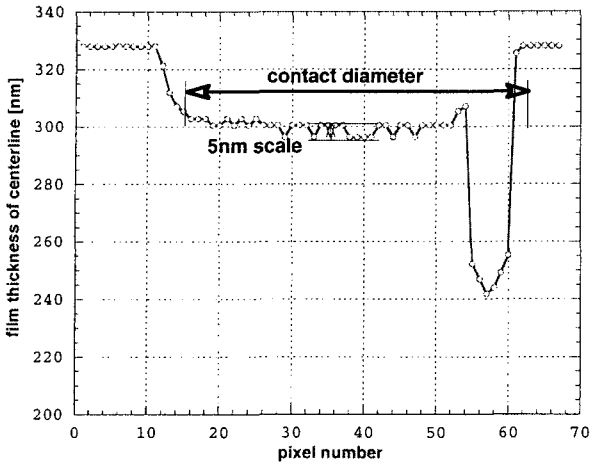

Figure 16 Centerline film thickness of base oil under the load of 15*N* and rolling speed of 0.03820*m/s* (Case II, Figure 11)

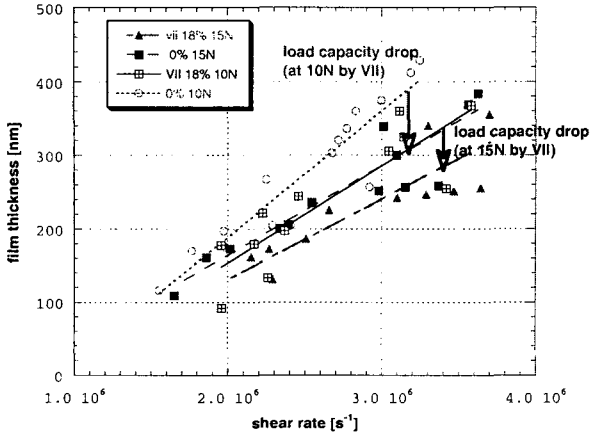

Figure 17 Minimum film thickness variations by changing applied loads, contact velocities and VII portion in base oil (Each line is linearly curve-fitted for the same loading condition and lubricant.)

5. CONCLUSION

In this work, optical interferometric measurement of EHL film thickness over the contact area is applied for the verification of load carrying performances of VII added lubricants, because it is possible only with fine resolution of length measurement of ~5*nm* scale. Theoretically, higher rolling contact velocity under the same applied load makes the EHL film thickness thicker for Newtonian lubricant without any exemption. However, for shear thinning lubricant such as VII blended lubricant, higher contact velocity under the same applied load makes the EHL film thickness delicately thinner comparing to that of Newtonian lubricant. Therefore, minute changes of EHL film thickness due to VII addition to base oil should be verified under various contact velocities and applied loads in order to find out the VII roles in synthesized lubricant.

With the developed image processing technology for EHL film thickness and in-situ measurement apparatus by the author, minute change of load carrying performance up to ~5*nm* in film thickness over the contact area can be verified for any kind of lubricants if it is under EHL contact regime. The load carrying capacities of some VII synthesized lubricant are tested and compared with Newtonian lubricant of base oil and it is found that the tested results agree well with theoretical tendencies.

ACKNOWLEGEMENT

본 연구는 한국과학재단 목적기초연구(2000-1-30400-005-3)지원으로 수행되었습니다.

REFERENCE

[1] Greenwood, J. A., 1988, "Film Thickness in Circular Elastohydrodynamic Contacts," Proc. Instn. Mech. Engrs. Vol. 202, No. C1, pp11-17.

[2] Hamrock, B. J., 1994, *Fundamentals of Fluid Film Lubrication*, McGraw-Hill.

[3] Johnston, G.J., Wayte, R. and Spikes, H.A., 1991, "The Measurement and Study of Very Thin Lubricant Films in Concentrated Contact," Tribology Transactions, Vol. 34, pp187-194.

[4] Ostensen, J. O., 1995, "Prediction of Film Thickness in an Elastohydrodynamic Point Contact Lubricated with a Viscosity Index Improved Base Oil," Proc. Instn. Mech. Engrs. Vol. 209, pp235-242.

[5] Evans, C. R., Jhonson, K. L., 1986, "The Rehological Properties of Elastohydrodynamic Lubricants," Proc. Instn. Mech. Engrs. Vol. 200, No. C5, pp303-312-17.

[6] Bair, S., 1995, "Elastohydrodynamic Film Forming with Shear Thinning Liquids," Journal of Tribology, vol. 120, pp.173-178.

[7] Williamson, B. P., 1995, "An Optical Study of Grease Rheology in an Elastohydrodynamic Point Contact under Fully Flooded and Starvation Conditions," Proc. Instn. Mech. Engrs. Vol. 209, pp63-74.

[8] Smeeth, M., Cann, P. M. and Spikes, H. A., 1995, "Measurement of Elstohydrodynamic Film Formation in Rolling Contacts at Very High Pressures," Lubricants and Lubrication, etited by Dowson, D., pp497-502, Elsevier

Science.

[9] Krupka, M., *et al.*, 1997, "Elastohydrodynamic Lubrication Film Shape – Comparison Between Experimental and Theoretical Results," Tribology for Energy Conservation, Elsevier, Amsterdam.

[10] Taylor, R I., 1997, "Engine Friction: the Influence of Lubricant Rheology," Proc. Instn. Mech. Engrs., Vol.211, Part J.

[11] Greenwood, J. A. and Kauslarich, J. J., 1997, "Elastohydrodynamic Film Thickness for Shear-Thinning Lubricants," Proc. Instn. Mech. Engrs., Vol. 212, Part J.

[12] Harris, J., 1977, Rheology and non-Newtonian Flow, Longman , New York.

[13] Bird, B., Armstrong, R., Hassager, O., 1987, Dynamics of Polymeric Liquids, John Wiley & Sons, New York.